arXiv:cond-mat/0403060v2 [cond-mat.mtrl-sci] 24 May 2005

Nonionic contributions to the electric-field gradient at ^{181}Ta and ^{111}Cd impurity sites in R_2O_3 (R= Sc, In, Lu, Yb, Tm, Er, Y, Ho, Dy, Gd, Eu, Sm) bixbyites

Leonardo A. Errico, Mario Rentería,* and Aníbal G. Bibiloni
Departamento de Física, Facultad de Ciencias Exactas,
Universidad Nacional de La Plata, C.C. 67, 1900 La Plata, Argentina.

Kristian Freitag
Helmholtz - Institut für Strahlen- und Kernphysik (ISKP),
Universität Bonn, Nussallee 14-16, 53115 Bonn, Germany

(Dated: February 2, 2008)

The time-differential perturbed-angular-correlation (TDPAC) technique was applied to the study of the internal electric-field gradient (EFG) in Eu- and Ho-sesquioxides in their cubic bixbyite phases. The results, as well as previous characterizations of the EFG at ^{181}Ta sites in oxides with the bixbyite structure, were compared to those obtained in experiments using ^{111}Cd as probe, and to point-charge model and *ab initio* results calculations for the EFG tensor at impurity sites in binary oxides. These studies provide quantitative information about electronic processes and the structural relaxations induced by the presence of impurity probes in the host lattices, and confirm the existence of nonionic contributions to the EFG in these systems. Our FP-LAPW calculations show that this nonionic contribution to the EFG is the dominating one, and that it is originated in the population of p states ($5p$ in the case of Cd, $6p$ for Ta).

PACS numbers: 61.72.Ww, 71.55.Ht, 81.05.Hd, 82.80.Ej

I. INTRODUCTION

During the last three decades, time-differential $\gamma-\gamma$ perturbed-angular-correlation (TDPAC) spectroscopy has been increasingly applied to condensed matter problems through the precise characterization of the electric-field-gradient (EFG) tensor at diluted (ppm) radioactive probe atoms, adequately introduced in substitutional host lattice sites (see, e.g., Refs. 1–3 and references therein). The characteristics of TDPAC allow carrying out the experiments under a wide range of suitable external conditions such as variable temperatures, pressures, atmospheres, etc. The single-atom counting of this technique, in combination with its highly localized sensitivity (due to the r^{-3} dependence of the electric-quadrupole interaction), allows a detailed investigation of both structural and electronic properties of the systems, providing information about crystal structures,[4] crystal chemistry,[5] defects,[6,7] nanoscopic characterizations of surfaces, interfaces,[8] and highly dispersed species[9,10], among other properties in solid state physics[11–18], chemistry and biology (see, e.g., Ref. 19, and references therein).

The very well suited (^{111}In $\rightarrow$)^{111}Cd isotope is the most frequently used tracer in TDPAC experiments and has been largely applied to study semiconductor physics. In particular, after the initial work of Pasquevich *et al.*[20] on the internal oxidation of diluted indium impurities in Ag, a large amount of experimental work has focused on the EFG characterization at ^{111}Cd impurity sites in semiconductor and insulating binary oxides.[21] All the information that the EFG tensor can provide about the system under study could be obtained by confrontation of the experiment with an accurate prediction of the EFG, such as those obtained with *ab initio* calculations. In the absence of such predictions at impurity sites, several attempts to correlate experimental results and semiempirical calculations have been made from the very beginning,[22,23] in order to describe the different contributions to the EFG at impurity sites.[24] In 1992, a well-defined empirical correlation between local (Cd valence states) and ionic contributions to the EFG was presented for ^{111}Cd in binary oxides.[25] In that analysis, the local component of the EFG in binary oxides was extracted from all quadrupole-coupling constants measured at that time in TDPAC experiments with the ^{111}Cd probe. The resulting systematics revealed a linear dependence between the local and ionic contributions to the EFG over a wide range of ionic EFG values. In 1994, Weht *et al.*[26] confirmed all the features of the correlation through an independent cluster calculation of the valence EFG contribution using the Extended Hüeckel Method. Recently, Errico *et al.*[27,28] reported the first *ab initio* full-potential linearized-augmented-plane-wave (FP-LAPW) calculations of the EFG at an impurity site (Cd) in an oxide (TiO_2), in excellent agreement with the experiments, supporting the existence of a dominant valence contribution to the EFG in this system, which can be identified with the local contribution of Ref. 25.

To study the influence of the electronic configuration of the impurity probe atom itself on the EFG it is essential to perform TDPAC measurements with different probes in isomorphus crystal structures. Examples of this kind of study are the work of Adams and Catchen,[5] and Shitu et al.[29] In TDPAC experiments, the second most commonly used radioactive probe is ^{181}Hf, which decays by β^- to the ^{181}Ta isotope. Therefore, in 1990 we started a comparative study of the EFG at ^{181}Ta and

^{111}Cd sites in binary oxides with the aim of investigating the EFG dependence on the electronic configuration of the probe atom and its coordination "chemistry" with its nearest neighbors.[30] Among the binary oxides, the sesquioxides that crystallize in the cubic bixbyite structure constitute a group widely studied with the ^{111}Cd probe.[11,12,31−35] This group presents interesting properties since it includes a large series of rare-earth as well as closed-shell metallic cations, a wide range of lattice constants (from 0.94 to 1.09 nm), and two nonequivalent cation sites with quite different symmetry, cation-oxygen bond lengths, and crystallographic abundance. These characteristics make this group ideally suited to study in detail the EFG dependence on the coordination geometry of the probe atoms and on their electronic configuration. With this purpose, in 1994 we started a systematic TDPAC study of this group using ^{181}Ta as probe.[36–41] From this systematic study and using the same hypothesis as in Ref. 25, we found an empirical correlation between the local and ionic contributions to the EFG similar to those found for ^{111}Cd, but with different slope.[39]

In this work we report TDPAC experiments using ^{181}Ta as probe in Eu_2O_3 and Ho_2O_3 in order to complete the systematic study of the EFG at ^{181}Ta atoms located at defect-free cation sites in the bixbyite structure. This systematics is compared to those previously established for the ^{111}Cd probe and to recent and new *ab initio* band-structure calculations of the EFG at impurity sites in a small set of binary oxides. This comparison provides quantitative information about electronic processes and the structural relaxations induced by the presence of impurity probes in the host lattices, information that cannot be obtained (or is crudely estimated) by simple models such as the point-charge model, the use of antishielding factors, and arbitrary suppositions. The *ab initio* calculations also predict the existence of a dominating nonionic (or local) contribution to the EFG originated from Cd-5*p* and Ta-6*p* states, in good agreement with the semiempirical model proposed in references 25 and 39. These new theoretical results, in combination with the experimental ones, enable us to discuss the validity of the widely used ionic model and to validate or discard the hypothesis used in the construction of the semiempirical model mentioned above and its predictions.

II. SAMPLE PREPARATION AND TDPAC MEASUREMENTS

Under suitable conditions, Fe, Mn, Sc, In, Tl, Y, and all the rare-earth elements form a sesquioxide. Polymorphism is common among the rare-earth oxides and below about 2300 K three polymorphous crystallographic structures have been found:[42] the hexagonal A-, the monoclinic B-, and the cubic C-form (bixbyite). In the cubic structure the cations form a nearly cubic face-centered lattice (space group Ia3) in which six out of the eight tetrahedral sites are occupied by oxygen atoms. The elementary cell of the oxide lattice consists of eight such cubes, containing 32 cations and 48 Oxygen ions. Two nonequivalent cationic sites, called C and D, both O_6-coordinated, characterize the structure. Their relative abundance in the lattice is $(f_C/f_D) = 3$. Site D is axially symmetric and can be locally described (see Fig. 1) as a cation surrounded by six oxygen atoms localized at the corners of a distorted cube, leaving two corners of a diagonal free (D_{3d} point-group symmetry). At site C the cube is more distorted (C_2-symmetry) and the six oxygen atoms leave two corners on a face diagonal free (see Fig. 1).

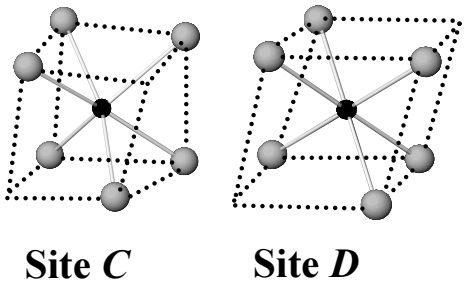

FIG. 1: Nearest-neighbor (NN) oxygen distribution around each cationic site (black atom) in the bixbyite structure.

In order to prepare the TDPAC samples, commercially obtained high-purity Ho_2O_3 and Eu_2O_3 powders (Aldrich Products, 99.9% and 99.95% metallic purity, respectively) were treated in air for 24 h at 1023 K in order to achieve the crystalline C-phase and then pressed as circular pellets under 20 kN/m^2 pressure. Afterward, the Ho_2O_3 pellet was sintered in air for 2.5 h at 1273 K whereas Eu_2O_3 was sintered under similar conditions but at 1123 K for 1.5 h because in this oxide the C-form presents a phase transition to the monoclinic B-phase at around 1353 K.[42] In both cases, powder XRD analyses of the samples performed before and after the sintering showed that only the C-phase was present and also revealed an increase in the crystallinity of the samples. The ion accelerator of the ISKP, Bonn, was then used to implant $^{181}Hf^+$ ions into the samples with the following energies and doses: Ho_2O_3, 160 keV, 5x10^{13} ions/cm^2 and Eu_2O_3, 155 keV, 5x10^{12} ions/cm^2. The as-implanted samples were subjected to TDPAC measurements in air at room temperature (RT = 300 K) and at atmospheric pressure. After these measurements the Ho_2O_3 and Eu_2O_3 samples underwent an annealing treatment in air at 1323 K and 1123 K for 2 h, respectively, since in other rare-earth sesquioxides annealing above 1073 K for a couple of hours has demonstrated to be sufficient to restore the host crystallinity and to locate the impurities at defect-free cationic sites. In the case of Ho_2O_3 the TDPAC measurements were then carried out in air in the temperature range RT-1373 K in 100 K steps.

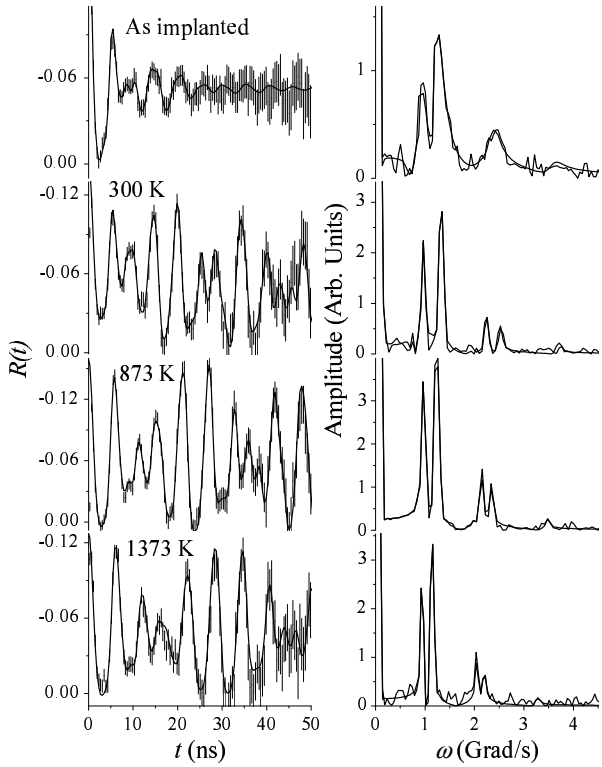

FIG. 2: $R(t)$ spectra (left) and their corresponding Fourier transforms (right) of (^{181}Hf→)^{181}Ta in Ho_2O_3 measured at RT in the as-implanted stage and at the indicated temperature after thermal annealing in air at 1323 K for 2 h.

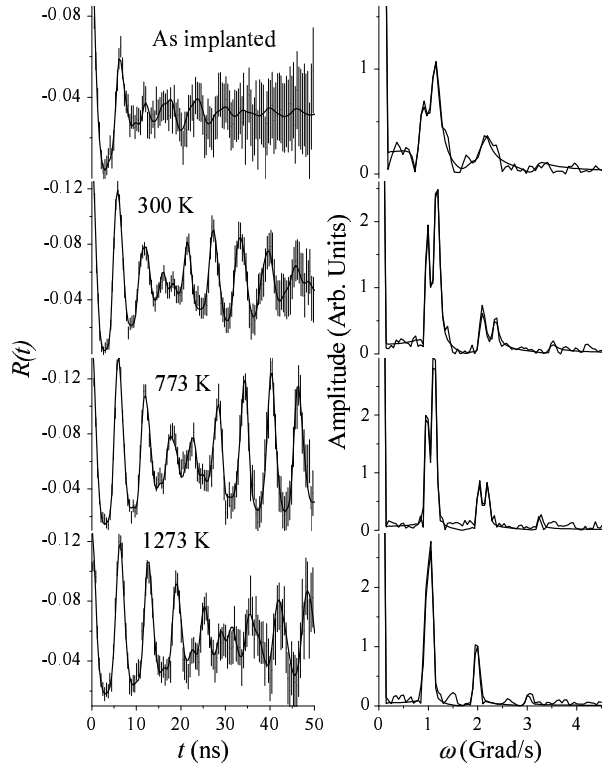

FIG. 3: $R(t)$ spectra (left) and their corresponding Fourier transforms (right) of (^{181}Hf→)^{181}Ta in Eu_2O_3 measured at RT in the as-implanted stage and at the indicated temperature after thermal annealing in air at 1123 K for 2 h.

In the case of Eu_2O_3 the measurements were performed between RT and 1273 K (in 100 K steps) and at 77 K.

The TDPAC technique is based on the determination of the influence of extranuclear fields on the correlation between the emission directions of two successive radiations emitted during a nuclear-decay cascade. A complete description of this technique can be found in the literature (see, e.g., Refs. 19 and 43). In order to perform the experiments presented in this work we made use of the well-known 133-482 keV $\gamma-\gamma$ cascade in ^{181}Ta, produced after the β^- nuclear decay of the ^{181}Hf isotope. The TDPAC experiments were made using four BaF_2 detectors in a coplanar 90° arrangement and a fast-fast logic coincidence system. The time and energy resolutions of the spectrometer for ^{181}Ta γ-rays are 0.65 ns (full width at half-maximum of the prompt peak) and 9.5% for γ-rays of 662 keV (^{137}Cs), respectively. The experimental perturbation functions, $R(t)$, were derived from eight concurrently measured coincidence spectra, four taken between detectors positioned with 180° symmetry and four of eight possible with 90° symmetry.[37] To analyze the measured perturbation functions, a multiple-site model for nuclear-electric-quadrupole interactions for polycrystalline samples and spin I=5/2 intermediate level of ^{181}Ta was used

$$R(t) = A_{22}^{exp} G_{22}(t) = \\ = A_{22}^{exp} \sum_i f_i S_{20,i} + \sum_{n=1}^{3} [S_{2n,i} \cos(\omega_{n,i} t) e^{-\delta_i \omega_{n,i} t}], \quad (1)$$

where f_i is the relative fraction of nuclei that experiences a given perturbation and A_{22}^{exp} is the effective anisotropy of the $\gamma-\gamma$ cascade. The ω_n interaction frequencies are related to the quadrupole frequency $\omega_Q = eQV_{ZZ}/40\hbar$ by $\omega_n = g_n \omega_Q$. The g_n and S_{2n} coefficients are known functions[44] of the asymmetry parameter $\eta = (V_{XX} - V_{YY})/V_{ZZ}$, where V_{ii} are the principal components of the EFG tensor that are arbitrarily labeled according to $|V_{XX}| < |V_{YY}| < |V_{ZZ}|$. The exponential functions in Eq. 1 account for a Lorentzian frequency distribution of relative width δ around ω_n.

III. ^{181}TA TDPAC RESULTS IN HO_2O_3 AND EU_2O_3

Figures 2 and 3 show the $R(t)$ spectra and their corresponding Fourier transforms, taken on both as-implanted samples at RT in air, and the selected spectra taken after

annealing of the samples. Solid lines in the $R(t)$ spectra are the best least-squares fits of Eq. 1 to the experimental data. Solid lines in the Fourier spectra come from the Fourier transform of the $R(t)$ fits. As can be seen from both figures, the as-implanted $R(t)$ spectra are rather damped, as usually occurs in the as-implanted stage of ^{181}Hf-implanted binary oxides,[36–38,40] showing that the radiation damage produces a not negligible host disorder around the probe atoms. After the annealing treatments, the radiation damage was removed in both samples. In effect, only two very well-defined ($\delta < 1.5\%$) hyperfine interactions (labeled Hfi C and Hfi D) were found, with the asymmetry parameter of Hfi D equal to zero and a high η value for Hfi C (see Table I) as predicted by the coordination symmetries of sites D and C, respectively. In addition, the frequency of the axially symmetric interaction is twice as large as the asymmetric one, as found previously with the ^{181}Ta probe in Yb-, Y-, Dy-, Sm-, Lu-, Gd-, Er- and Tm-sesquioxides.[36−41] The asymmetry parameters and distributions of Hfi C and Hfi D for both oxides are constant with temperature, while the quadrupole frequencies show a reversible continuous decrease with increasing temperature in the measured temperature range. The monotonic trend of the hyperfine parameters of Hfi C and Hfi D is a typical behavior followed by hyperfine probes in substitutional cation sites of a single-phase crystalline structure. The total fraction of both interactions amounts to 100% of the probes in the whole temperature range of measurement for Eu_2O_3. This statement also applies to Ho_2O_3, with the exception that two minor interactions amount to less than 20% of the probes in the temperature range RT-472 K. The relative population of the two sites should be $(f_C/f_D) = 3$ if the cationic sites were occupied according to their natural abundance in the crystalline structure. In the present experiments, $(f_C/f_D) = 3$ was found for Eu_2O_3. In the case of Ho_2O_3, the experimental ratio f_C/f_D was smaller than this value. This departure was already observed for (^{181}Hf→)^{181}Ta in other bixbyites and was explained in terms of the relative ionic size of the probe and the cationic "space" of the host.[37,38] The present results for Ho- and Eu-sesquioxides are in excellent agreement with the occupancy trend previously observed (see Fig. 4). It is then clear that Hfi C and Hfi D can be undoubtedly assigned to probes located at the crystalline nonequivalent cationic sites C and D.

We want to mention that the f_C/f_D ratio for Ho_2O_3 and Eu_2O_3 obtained with ^{181}Ta, as well as those for the rest of the bixbyite series, is independent of the sample temperature (in the range RT-1300 K). This may be evidence of no further ionic transport after the annealing process.

The two minor frequencies observed for Ho_2O_3 exist in a short temperature range and disappear above 573 K in a reversible way. Due to the temperature range in which these minor interactions exist we have investigated the possibility of desorption-absorption of water in the samples. However, a Differential-Thermal Analysis (DTA) carried out for the Ho_2O_3 samples did not confirm this hypothesis.

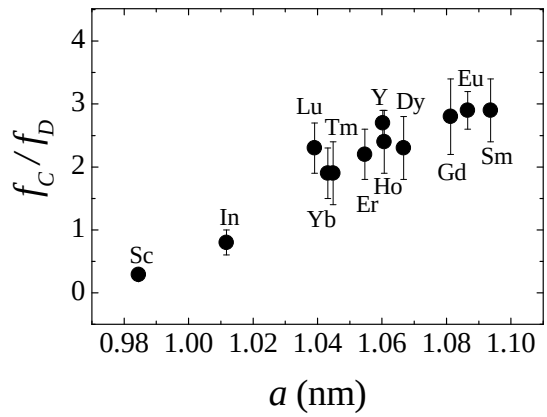

FIG. 4: Experimental ratio f_C/f_D as a function of the lattice parameter a for ^{181}Ta in bixbyites.

IV. DISCUSSION

A. Systematics of the EFG at ^{111}Cd and ^{181}Ta impurity sites in bixbyites

In 1994, we started a TDPAC study of the EFG dependence on the probe atom in bixbyites, measuring the EFG at ^{181}Ta impurity sites in Yb-, Y-, and Dy-sesquioxides,[36] In_2O_3,[37] Sc_2O_3 and Sm_2O_3,[38,39] Lu_2O_3,[39] Er_2O_3 and Gd_2O_3,[40] and Tm_2O_3.[41] Including the new data presented in this paper, i.e., Eu_2O_3 and Ho_2O_3, we can now compare a set of twelve oxides, all having the same crystalline structure, but differing in their lattice constant by 10%. In Fig. 5 we present the values of ω_Q and η for both sites as a function of the lattice parameter a. All the experimental data in this figure (and also in Fig 4) correspond to TDPAC experiments in which the ^{181}Hf isotope was introduced into the samples by means of ion implantation, with the exception of Tm_2O_3. In this case the activity was introduced by means of a solid-state reaction assisted by ball milling between powders of Tm-sesquioxide and neutron-activated HfO_2. In spite of the limited accuracy of the derived hyperfine parameters in this experiment, due to a remaining 40% fraction of probes located in a highly distorted HfO_2 phase, the hyperfine interaction parameters corresponding to Tm_2O_3 appear to be reliable considering their excellent agreement with the rest of the systematics. As can be seen in Fig. 5, there is a jump in the ^{181}Ta systematics. In effect, ω_{QC} and ω_{QD} for Sc_2O_3 and In_2O_3 (the sesquioxides with the smallest lattice parameters) depart from the linear dependence on a shown by the rest of the sesquioxides. Concerning the asymmetry parameter, while η_D is nearly independent of a for all the measured sesquioxides and close to 0, η_C does not show an increase with

TABLE I: Results of least-squares fits of Eq. 1 to the $R(t)$ spectra displayed in Figs. 2 and 3, taken at RT after annealing. f_i and δ_i are expressed in % and ω_{Qi} in Mrad/s. When no errors are quoted it means that the parameter was kept fixed in order to evaluate errors. In the case of Ho_2O_3 the fractions $f_C + f_D$ are normalized to 100% (see text).

	Hfi C				Hfi D			
	f	ω_Q	η	δ	f	ω_Q	η	δ
Ho_2O_3	70(4)	114.3(3)	0.612(4)	0.0(2)	30(5)	207.0(7)	0	0.3(4)
Eu_2O_3	74(8)	101.2(3)	0.798(4)	1.6(4)	26(3)	193.8(9)	0	1(1)

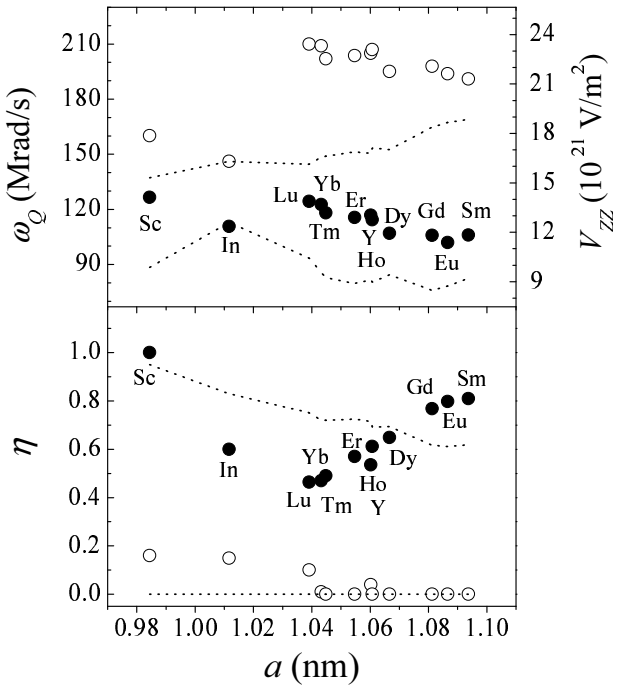

FIG. 5: Experimental quadrupole frequency ω_Q and asymmetry parameter η for substitutional ^{181}Ta impurities at sites C (black) and D (hollow) in bixbyites plotted as a function of the lattice parameter a at RT. To obtain V_{zz} from ω_Q we used $Q_{Ta} = (+)2.36(5)$ b.[45] The errors are smaller than the symbols. Dotted lines are the PCM predictions. The ω_Q predictions are normalized to the In_2O_3 values.The lattice parameters and the atomic coordinates used in the PCM calculations for each oxide have been taken from neutron and x-ray diffraction (XRD) determinations quoted in the literature.[46]

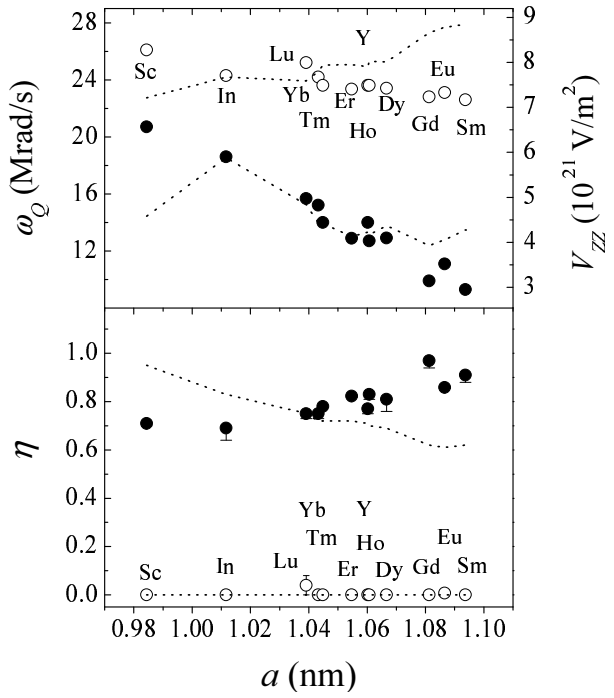

FIG. 6: Experimental quadrupole frequency ω_Q and asymmetry parameter η for substitutional ^{111}Cd impurities at sites C (black) and D (hollow) in bixbyites[11,12,31−35] plotted as a function of the lattice parameter a at RT. The results for Lu_2O_3 and Tm_2O_3 correspond to 1273 and 583 K, respectively (see Refs. 11 and 35). In order to obtain V_{zz} from ω_Q we used $Q_{Cd} = (+)0.83(13)$ b .[47] The errors are smaller than the symbols. Dotted lines are the PCM predictions. The ω_Q predictions are normalized to the In_2O_3 values.

a for In- and Sc-sesquioxides, as occurs for the rest of the systematics (see Fig. 5). The anomalous behavior of the ω_Q and η_C parameters may indicate the presence of structural distortions in the host lattice induced by the impurity. We will discuss this statement in the next section.

If we compare the trend of ω_Q and η with point-charge model (PCM) predictions (see Fig. 5), we find that the observed increase of η_C and the dependence of ω_{QC} and ω_{QD} on a are in poor agreement. At this point it is necessary to analyze the experimental hyperfine interaction parameters at ^{111}Cd impurity sites in bixbyites reported in the literature.[11,12,31−35] Figure 6 shows a monotonic dependence of the hyperfine parameters ω_Q and η on the lattice parameter a for both sites. These trends are in poor agreement with those predicted by the PCM, as can be seen in the same figure. In the past, this discrepancy was explained by two different approaches. In the first one,[33,48] the PCM was considered accurate enough to exactly predict the hyperfine parameters that characterize the EFG at Cd sites in bixbyites. In this model, the EFG is given by

$$V_{ZZ}^{ionic} = (1 - \gamma_\infty) V_{ZZ}^{latt}, \quad (2)$$

where γ_∞ is the Sternheimer antishielding factor and, in the principal axes system:

$$V_{ZZ}^{latt} = \frac{e}{4\pi\varepsilon_0} \sum_k Z_k \frac{3x_{ki}x_{kj} - \delta_{ij} r_k^2}{r_k^5}. \quad (3)$$

In the above expression, Z_k denotes the (arbitrary) ionic charge, x_{ki} and x_{kj} the coordinates, and r_k the distance of the kth ion to the site where the EFG is calculated, located at the origin of the coordinated system for simplicity. The discrepancy between PCM predictions and the experimental results was attributed to a wrong determination of the atomic positions in these compounds (mainly the oxygen atoms). Within this framework, the authors of Refs. 33 and 48 used the PCM to refine the atomic positions in order to reproduce the experimental EFG results. It is worthy of mention that that approach presented several assumptions, e.g., pure ionic bonding between the probe atom and its neighbors was assumed and local lattice distortions caused by the ^{111}Cd impurity were not considered. At this point, it is important to mention that that model was proposed before a ^{181}Ta systematics in bixbyites was established. Now, the very different trend between the experimental ^{181}Ta data presented here and the PCM predictions with the refined coordinates of Ref. 48 gives clear evidence of the failure of this model in the ^{181}Ta case and makes its applicability suspicious in the ^{111}Cd one. In the next section, we present theoretical evidence that supports this statement.

The second approach was first proposed to describe the whole set of EFG results at ^{111}Cd in binary oxides in a unified way,[25] and then it was extended to the ^{181}Ta impurity. Since this model was constructed to exactly reproduce the magnitude of all the existent experimental EFG results, the hypothesis involved in it and the predictions of this model for the sign of V_{zz} (opposite to those of V_{ZZ}^{ionic}, see Ref. 25) have to be discussed now, enlightened by the first-principles predictions, which were not available at the time the model was proposed. In this approach, Rentería et al.[24,25] proposed the existence of a dominating local contribution to the EFG. In this model the EFG is given by

$$V_{ZZ} = V_{ZZ}^{local} + (1 - \gamma_\infty) V_{ZZ}^{latt}. \quad (4)$$

The local contribution to the EFG takes into account covalence between the probe and its neighbors. From the study of the experimental EFG results at ^{111}Cd and ^{181}Ta impurity sites in binary oxides we demonstrated that, for both probes, V_{ZZ}^{local} shows an almost linear dependence on V_{ZZ}^{ionic} (see Ref. 39). We also demonstrated that V_{ZZ}^{local} can be factorized in two parts, one that depends on the geometry of the cationic site and another that depends on the electronic configuration of the probe, thus[39,40]

$$\begin{aligned} V_{ZZ}(site\ i, probe\ i) &= \mu^{probe\ i}(1-\gamma_\infty)^{probe\ i} \\ &\times\ \mu^{geometry}\ V_{ZZ}^{latt}(site\ i). \quad (5) \end{aligned}$$

We must say here that this semiempirical model is still based on point-charge summations and takes into account the contribution of the electronic structure of the probe to the EFG by means of antishielding factors and empirical parameters (such as μ^{probe} and $\mu^{geometry}$). Moreover, this model does not take into account possible effects introduced by the impurity character of the probe, such us lattice distortions. Nevertheless, this simple semiempirical model has been successfully used as a tool for the assignment of hyperfine interactions in complex systems.[16] In the next section the hypothesis and predictions of this model are discussed in terms of very recent band-structure FP-LAPW calculations of the EFG at Cd and Ta impurity sites in In_2O_3 and other binary oxides.

B. FP-LAPW results for the EFG tensor at impurity sites in binary oxides

Since this paper deals with the EFG at impurity sites, the interpretation of the experimental results involves the understanding of chemical differences between the probe atom and the indigenous ion replaced by the impurity. The experimental results show that the differences between probes and indigenous atoms are manifest in subtle ways that are not well described by conventional models, as already pointed out in Ref. 5. For an accurate calculation of the EFG, the electronic configuration of the host, perturbed by the presence of the impurity, has to be determined. This can be done in the framework of the Density-Functional Theory (DFT). In this kind of calculation, electronic and structural effects introduced in the host by the presence of the impurity probe (impurity levels, structural distortions, etc.) can be described without the use of arbitrary suppositions. Unfortunately, these calculations prove to be not trivial and time-consuming. For this reason, very few calculations have been performed in systems with impurities and the method is far from being routinely applied in this field.[27,28] Moreover, the applicability of the DFT to bixbyites that contain rare earth cations is not clear yet since the $4f$-valence electrons are not well described by this theory.[49]

In the last years we performed FP-LAPW[50] calculations in the systems TiO_2(Cd),[27,28] SnO_2(Cd),[51] TiO_2(Ta), and SnO_2(Ta).[52] We present here new calculations of the EFG tensor at Cd and Ta impurities that replace cations in the model case In_2O_3. For the calculations we employed the Wien97.10 implementation[53] of the FP-LAPW method within the Generalized Gradient Approximation (GGA) for the exchange-correlation potential.[54] For the parameter RK_{MAX}, which controls the size of the basis set, we took the value of 7 and introduced local orbitals for In-4d and 4p, O-2s, Cd-4d and 4p, and Ta-6s, 5p, and 4f orbitals. With these parameters, the convergence errors in the V_{ii} components are smaller than 0.1×10^{21}V/m^2. In the case of the

asymmetry parameter η, the convergence error is smaller than 0.05. In order to study the structural distortions introduced by the impurity in the host we considered the displacements of the impurity nearest oxygen neighbors until forces acting on these atoms vanished, assuming that structural distortions preserve the point-group symmetry of the cell in its initial configuration. Due to the large number of atoms in the unit cell of In_2O_3, we did not use a super-cell approach for the simulation of the isolated impurity. Details of the method of calculation and the way to deal with the impurity were extensively explained in Refs. 27 and 28. It is clear that, even including the new FP-LAPW results reported here, the number of EFG calculations at impurity sites is very small to perform a systematic study, but some important conclusions can be drawn.

The first important theoretical result is that in all the studied systems the impurity probes introduce local distortions in the host. It is worthy of mention that in all the cases the amount of distortion per atom decreases rapidly from the impurity nearest oxygen neighbors (O_{NN}) to other shells. In the case of Cd located at both cationic sites of In_2O_3 we found that the impurity produced relaxations of about 5% (see Table II) of the cadmium O_{NN}. Additionally, in the case of Cd located at site C we found that the impurity moved out from the symmetry site, but this displacement (3x10^{-4} nm) is very small compared to the displacement of the Cd O_{NN}. Larger relaxations were also found in TiO_2 and SnO_2 for the Cd impurity. These relaxations can be understood from the fact that the bond length of the sixfold coordinated Cd ion in CdO is about 0.235 nm. It seems that the local structure of the Cd impurity tries to reconstruct the environment of Cd in its own oxide.[51,52] Since in the rest of the bixbyites most of the bond lengths are smaller than 0.235 nm, one could also expect relaxations around the Cd impurity site in all of them. The presence of these structural relaxations in bixbyites with Cd shows that the refinement proposed in Refs. 33 and 48 is not valid since it is based on the fact that the Cd impurity does not introduce structural distortions in the host. In this sense this model mistakes a local effect (the O_{NN} relaxations originated by the impurity character of the probe) for a pretended wrong determination of the host atomic positions by XRD, which involves all the lattice.

In the case of Ta at site D of In_2O_3, we found that Ta induces a 7% contraction in the Ta-O_{NN} distance. Calculations at site C predict 5-10% contractions of the Ta-O_{NN} distances (see Table II) and a negligible displacement of Ta from the symmetry site. We have also found contractions in the case of SnO_2(Ta), whereas in TiO_2(Ta) the local structural distortions are negligible.[52] These contractions can be understood from the fact that the bond lengths of the sixfold coordinated Ta ion in TaO_2 are about 0.202 nm. As in the case of Cd, it seems that the local structure tries to reconstruct the environment of Ta in its oxide. Due to the larger bond lengths of the rest of the bixbyites we should also expect contractions of the Ta-O_{NN} distances. From these considerations it is clear that distortions with different symmetry and/or magnitude for In- and Sc-sesquioxides with respect to those of the rest of the systematics could be at the origin of the anomalous behavior of the hyperfine parameters for Ta in bixbyites shown in Fig. 5.

We can discuss now the FP-LAPW predictions for the EFG tensor and compare them with the experiments, the PCM, and the semiempirical model of Ref. 39. From our calculations we found that relaxations (or contractions) beyond the O_{NN} shell do not produce qualitative changes in the EFG tensor. For this reason all the FP-LAPW results for the EFG tensor shown here correspond to the relaxed position of the O_{NN}. There is an excellent agreement between the experiments and FP-LAPW predictions for the EFG at Cd impurity sites, as shown in Table III. On the other hand, the PCM fails completely in the description of the EFG for TiO_2. The agreement is better for SnO_2, but the PCM fails in the prediction of the asymmetry parameter. This failure should be expected due to their covalency originated in the short Cd-O_{NN} bond lengths. In the case of In_2O_3, where the bond lengths are larger, the PCM agrees with the FP-LAPW EFG prediction for Cd at site D, but disagrees in the sign of the major component of the EFG tensor for Cd at site C.

In the case of the Ta impurity, the agreement between the experiments and FP-LAPW predictions is very good, with exception of Ta at site C in In_2O_3. Here it is important to say that due to the hypothesis used in the relaxation process (structural relaxations preserve the point-group symmetry of the cell in its initial configuration), FP-LAPW cannot reproduce the small departure from the axial symmetry experimentally observed for Ta at site D of In_2O_3 (see Table III). On the other hand, the PCM fails completely in the description of the EFG at Ta impurities located at cationic sites of TiO_2 and SnO_2. In the case of the EFG at Ta impurities located at sites C and D of In_2O_3, the PCM agreement with the available experimental data (V_{ZZ} and η) is better than that of the FP-LAPW predictions. Hence, from eight probe-oxygen configurations, five are not well described by the PCM.

The *ab initio* calculations predicted local distortions in almost all the cases studied. If we use the relaxed positions of the O_{NN} atoms predicted by FP-LAPW in the PCM calculations, this model still fails in the predictions of the EFG. Moreover, in most of the cases the disagreement becomes worse. From this discussion it is clear now that the failure of the PCM prediction of the EFG at impurity sites is not only due to the use of wrong atomic positions but to a wrong description of the electronic structure of the impurity-host system, in particular in the vicinity of the impurity.

Based on the FP-LAPW calculations we can finally discuss the validity of the hypothesis on which the semiempirical model is based, i.e., the existence of a dominating local contribution to the EFG. In this model, the EFG can be written as

TABLE II: Experimental and FP-LAPW-refined In-O distances (in nm) in pure In_2O_3 compared with the relaxed Cd-O and contracted Ta-O distances (last two rows) calculated when a Cd or a Ta atom replaces an In atom in In_2O_3.

	Site D		Site C	
	$d(In-O)$	$d(In-O1)$	$d(In-O2)$	$d(In-O3)$
Pure In_2O_3 (Experimental)[55]	0.219(2)	0.212(2)	0.219(1)	0.221(2)
Pure In_2O_3 (FP-LAPW, this work)	0.218	0.213	0.219	0.223
In_2O_3:Cd (FP-LAPW, this work)	0.227	0.220	0.229	0.233
In_2O_3:Ta (FP-LAPW, this work)	0.202	0.197	0.197	0.209

TABLE III: Experimental EFG results available for TiO_2, SnO_2, and In_2O_3 doped with Cd and Ta compared with the PCM and FP-LAPW predictions. The signs of V_{ZZ} at the Cd and Ta sites are not known experimentally.

System	Method	V_{ZZ}	V_{ZZ} direction	η
$TiO_2 : Cd$	PCM	-2.21	$[1\bar{1}0]$	0.43
	FP-LAPW[28]	$+4.55$	[110]	0.26
	Experimental[27]	5.34(1)	[110] or $[1\bar{1}0]$	0.18(1)
$SnO_2 : Cd$	PCM	$+5.21$	[110]	0.40
	FP-LAPW[51]	$+5.35$	[110]	0.10
	Experimental[56]	5.83(4)	-	0.18(2)
In_2O_3:Cd (Site D)	PCM	$+7.5$	[111]	0.00
	FP-LAPW (this work)	$+7.6$	[111]	0.00
	Experimental[13]	7.7(1)	[111][a]	0.00(5)
In_2O_3:Cd (Site C)	PCM	-4.9	$[0\bar{0}.7\bar{5}1]$	0.83
	FP-LAPW (this work)	$+5.6$	$[0\bar{0}.7\bar{5}1]$	0.68
	Experimental[13]	5.9(1)	$[0\bar{1}1]$[a]	0.69(1)
TiO_2:Ta	PCM	-4.55	$[1\bar{1}0]$	0.43
	FP-LAPW[52]	-13.0	[001]	0.69
	Experimental[57]	13.3(1)	[001]	0.56(1)
SnO_2:Ta	PCM	$+10.76$	[110]	0.40
	FP-LAPW[51]	-17.7	[001]	0.96
	Experimental[30]	17.04(1)	-	0.70(2)
In_2O_3:Ta (Site D)	PCM	$+15.46$	[111]	0.00
	FP-LAPW (this work)	$+19.7$	[111]	0.00
	Experimental[37]	16.31(2)	-	0.149(7)
In_2O_3:Ta (Site C)	PCM	-10.10	$[0\bar{0}.7\bar{5}1]$	0.83
	FP-LAPW (this work)	-17.8	[010.3]	0.26
	Experimental[37]	12.35(9)	-	0.60(9)

[a] Experimental values obtained with ^{111}Cd in Er_2O_3 and Ho_2O_3 single crystals.[33]

$$V_{ZZ} = V_{ZZ}^{local} - \gamma_\infty V_{ZZ}^{latt(PCM)} + V_{ZZ}^{latt(PCM)}, \qquad (6)$$

meanwhile in the FP-LAPW framework we have

$$V_{ZZ}^{LAPW} = V_{ZZ}^{val} + V_{ZZ}^{latt(LAPW)} = \\ = V_{ZZ}^{val,p} + V_{ZZ}^{val,d} + V_{ZZ}^{latt(LAPW)}, \qquad (7)$$

where $V_{ZZ}^{val,p}(V_{ZZ}^{val,d})$ is the valence contribution of Cd- or Ta-p(d) orbitals inside the muffin-tin sphere of the impurity and $V_{ZZ}^{latt(LAPW)}$ is the total contribution originated in the charge density outside that sphere.

In both cases (Eqs. 6 and 7) the lattice contributions are negligible. Taking into account the d orbitals involved in the γ_∞ factor ($4d$ for Cd, $5d$ for Ta), we can correlate the term -$\gamma_\infty V_{ZZ}^{latt(PCM)}$ of Eq. 6 with the d valence contribution to the EFG in FP-LAPW calculations (Eq. 7). In this way, the p valence contribution of Eq. 7 has to be correlated with V_{ZZ}^{local} in Eq. 6. With this "bridge" linking both models, we can return to the results obtained in the FP-LAPW calculations. In all the studied systems (including In_2O_3) and for both probes we found that the p contribution ($5p$ in the case of Cd, $6p$ for Ta) dominates over the d contribution. Based on these results, we can conclude that the *ab initio* calculations of the EFG tensor at impurity sites support the hypothesis of the existence of a local and dominating contribution to the EFG on which the semiempirical model is based. This model gives a better qualitative description of the EFG than the PCM because it includes a contribution to the EFG that is not taken into account in the PCM. But the semiempirical model is based on the use of the

γ_∞ factor and point-charge summations that do not take into account the structural distortions introduced by the impurity. These shortcomings could produce wrong predictions in our model, such as the wrong prediction of the EFG sign in various of the compounds shown in Table III. An extensive first-principles study of the EFG at impurity sites in binary oxides is essential in order to remove these shortcomings.

V. CONCLUSIONS

In order to compare complete sets of EFGs at ^{181}Ta and ^{111}Cd sites in bixbyite oxides we determined the electric-quadrupole hyperfine interactions at ^{181}Ta impurities in Eu_2O_3 and Ho_2O_3. Including previous results, we could compare a set of twelve oxides having the same crystalline structure. Our study shows that in all these oxides, after the implantation and subsequent high-temperature annealing, the probes ^{181}Hf occupy two sites that have been identified as the two nonequivalent cation sites of the bixbyite structure. We confirm a jump in the values of ω_{QC} and ω_{QD} that takes place for $a < 1.0391$ nm, that is for lattice parameters smaller than that of Lu-sesquioxide. Concerning the asymmetry parameter, while $\eta_D \approx 0.0$ is nearly independent of a for all the measured sesquioxides, η_C for indium and scandium sesquioxides departs from the tendency that rules its behavior for the rest of the systematics. These anomalous experimental behaviors, in combination with our FP-LAPW predictions for Ta in In_2O_3 (and in the other binary oxides), suggest that Ta induces contractions of its O_{NN} in all the bixbyites, but with different symmetry and/or magnitude in the case of In_2O_3 and Sc_2O_3.

The experimental EFG data obtained at ^{111}Cd and ^{181}Ta impurity sites in binary oxides available at present clearly show that a single ionic model cannot describe the EFG, suggesting the existence of a dominating non-ionic contribution as stated in the semiempirical model. This assertion is supported by our band-structure FP-LAPW calculations at Cd and Ta impurity sites in binary oxides, which show that the dominating contribution to the EFG is originated in Cd-5p and Ta-6p states, respectively. These results can now explain the dependence of the local EFG, proposed in the semiempirical model, on the electronic configuration of the probes. Future FP-LAPW calculations, currently in progress, at impurity sites in oxides and, in particular, in bixbyites, will certainly go deeper into the understanding of structural and electronic properties at impurity sites in semiconducting oxides.

Acknowledgments

It is a pleasure to recognize our colleague Prof. Dr. Patricia Massolo, who shared with us the motivations of this research. We greatly appreciate the valuable suggestions of Dr. R. Vianden and Dr. T. Butz during the design of the detectors and the acquisition of spare parts of the TDPAC spectrometer. This work was partially supported by Agencia Nacional de Promoción Científica y Tecnológica (ANPCyT) under PICT98 03-03727, Consejo Nacional de Investigaciones Científicas y Técnicas (CONICET) under PIP006/98, and Fundación Antorchas, Argentina, and the Third World Academy of Sciences (TWAS), Italy, RGA 97-057. The neutron irradiations performed by the GKSS reactor FRG-1, Germany, are kindly acknowledged. M.R., L.A.E, and A.G.B. are members of CONICET, Argentina.

* Correspondace should be addressed to: `renteria@fisica.unlp.edu.ar;errico@fisica.unlp.edu.ar`

[1] E. N. Kaufmann and R. J. Vianden, Rev. Mod. Phys. **51**, 161 (1979).
[2] A. Lerf and T. Butz, Hyperfine Interact. **36**, 275 (1987).
[3] A. R. López-García, Magn. Res. Rev. **15**, 119 (1990).
[4] D. Lupascu, M. Uhrmacher, and K. P. Lieb, J. Phys.: Condens. Matter **6**, 10445 (1994).
[5] J. M. Adams and G. L. Catchen, Phys. Rev. B **50**, 1264 (1994).
[6] S. Lany, P. Blaha, J. Hamann, V. Ostheimer, H. Wolf, and T. Wichert, Phys. Rev. B **62**, R2259 (2000); T. Wichert and S. Lany, Hyperfine Interact. **136/137**, 453 (2001).
[7] N. Mommer, T. Lee, J. A. Gardner, and W. E. Evenson, Phys. Rev. B **61**, 162 (2000).
[8] T. Klas, J. Voigt, W. Keppner, R. Wesche, and G. Schatz, Phys. Rev. Lett. **57**, 1068 (1986); R. Fink, T. Koch, G. Krausch, J. Marien, A. Plewnia, B. U. Runge, G. Schatz, A. Siber, and P. Ziemann, Phys. Rev. B **47**, R10048 (1993).
[9] J. M. Ramallo-López, M. Rentería, E. E. Miró, F. G. Requejo, and A. Traverse, Phys. Rev. Lett. **91**, 108304 (2003).
[10] A. F. Pasquevich, F. H. Sánchez, A. G. Bibiloni, J. Desimoni, and A. López-García, Phys. Rev. B **27**, 963 (1983); J. Desimoni, A. G. Bibiloni, L. Mendoza-Zélis, A. F. Pasquevich, F. H. Sánchez, and A. López-García, Phys. Rev. B **28**, 5739 (1983).
[11] L. A. Errico, M. Rentería, A. G. Bibiloni, and F. G. Requejo, Hyperfine Interact. **120/121**, 457 (1999).
[12] A. G. Bibiloni, J. Desimoni, C. P. Massolo, L. Mendoza-Zélis, A. F. Pasquevich, F. H. Sánchez, and A. López-García, Phys. Rev. B **29**, R1109 (1984).
[13] S. Habenicht, D. Lupascu, M. Uhrmacher, L. Ziegeler, K. P. Lieb, and ISOLDE Collaboration, Z. Phys. B **101**, 187 (1996).
[14] N. Achtziger and W. Witthuhn, Phys. Rev. B **47**, 6990 (1993).
[15] R. Vianden and U. Feuser, Phys. Rev. Lett. **61**, 1981 (1988).
[16] M. Rentería , L. A. Errico, A. G. Bibiloni, K. Freitag, and F. G. Requejo, Z. Naturforsch. A **55**, 155 (2000).
[17] M. Forker, S. Muller, P. de la Presa, and A. F. Pasquevich Phys. Rev. B **68**, 14409 (2003).

[18] J. Meersschaut, C. Labbe, M. Rots, and S. D. Bader, Phys. Rev. Lett. **87**, 107201 (2001).

[19] A. Lerf and T. Butz, Angew. Chem. Int. Ed. Engl. **26**, 110 (1987).

[20] A. F. Pasquevich, A. G. Bibiloni, C. P. Massolo, F. H. Sánchez, and A. López-García, Phys. Lett. A **82**, 34 (1981).

[21] See, for example, D. Wiarda, M. Uhrmacher, A. Bartos, and K. P. Lieb, J. Phys.: Condens. Matter **5**, 4111 (1993); M. Neubauer, A. Bartos, K. P. Lieb, D. Lupascu, M. Uhrmacher, and Th. Wenzel, Europhys. Lett. **29**, 175 (1995); J. Luthin, K. P. Lieb, M. Neubauer, M. Uhrmacher, and B. Lindgren, Phys. Rev. B **57**, 15272 (1998), and references therein.

[22] W. Bolse, A. Bartos, J. Kesten, M. Uhrmacher, and K. P. Lieb, XXIII Zacopane School on Physics, edited by K. Krolas and K. Tomala (Institute of Nuclear Physics, Cracow, 1988).

[23] J. Kesten, W. Bolse, K. P. Lieb, and M. Uhrmacher, Hyperfine Interact. **60**, 683 (1990).

[24] M. Rentería, Ph.D. thesis, Universidad Nacional de La Plata, Argentina, 1992.

[25] M. Rentería, C. P. Massolo, and A. G. Bibiloni, Mod. Phys. Lett. B **6**, 1819 (1992).

[26] R. Weht, G. Fabricius, M. Weissmann, M. Rentería, C. P. Massolo, and A. G. Bibiloni, Phys. Rev. B **49**, 14939 (1994).

[27] L. A. Errico, G. Fabricius, M. Rentería, P. de la Presa, and M. Forker, Phys. Rev. Lett. **89**, 55503 (2002).

[28] L. A. Errico, G. Fabricius, and M. Rentería, Phys. Rev. B **67**, 144104 (2003).

[29] J. Shitu, A.F. Pasquevich, A.G. Bibiloni, M. Rentería, F.G. Requejo, Mod. Phys. Lett. B **12**, 281 (1998).

[30] M. S. Moreno, J. Desimoni, A. G. Bibiloni, M. Rentería, C. P. Massolo, and K. Freitag, Phys. Rev. B **43**, 10086 (1991).

[31] A. Bartos, K. P. Lieb, A. F. Pasquevich, M. Uhrmacher, and ISOLDE collaboration, Phys. Lett. A **157**, 513 (1991).

[32] J. Shitu, D. Wiarda, Th. Wenzel, M. Uhrmacher, K. P. Lieb, S. Bedi, and A. Bartos, Phys. Rev. B **46**, 7987 (1992).

[33] D. Lupascu, A. Bartos, K. P. Lieb, and M. Uhrmacher, Z. Phys. B **93**, 441 (1994).

[34] A. F. Pasquevich, A. M. Rodríguez, H. Saitovich, and P. R. de Jesus-Silva, private communication.

[35] A. W. Carbonari, J. Mestnik-Filho, R. N. Attili, M. Moralles, and R. N. Saxena, Hyperfine Interact. **120/121**, 475 (1999).

[36] A. F. Pasquevich, A. G. Bibiloni, C. P. Massolo, M. Rentería, J. A. Vercesi, and K. Freitag, Phys. Rev. B **49**, 14331 (1994).

[37] M. Rentería, F. G. Requejo, A. G. Bibiloni, A. F. Pasquevich, J. Shitu, and K. Freitag, Phys. Rev. B **55**, 14200 (1997).

[38] M. Rentería, A. G. Bibiloni, F. G. Requejo, A. F. Pasquevich, J. Shitu, L. A. Errico, and K. Freitag, Mod. Phys. Lett. B **12**, 819 (1998).

[39] M. Rentería, K. Freitag, and L. A. Errico, Hyperfine Interact. **120/121**, 449 (1999).

[40] L. A. Errico, M. Rentería, A. F. Pasquevich, A. G. Bibiloni, and K. Freitag, Eur. Phys. J. B **22**, 149 (2001).

[41] G. N. Darriba, L. A. Errico, and M Rentería, in *Anales AFA 14*, proceedings of the 87th Reunión Nacional de Física, Huerta Grande, 2001, p. 208, edited by Asociación Física Argentina (Universidad Nacional del Centro,Tandil, 2002).

[42] L. Eyring, in *Handbook on the Physics and Chemistry of Rare Earths*, edited by K. A. Gschneidner and L. Eyring (North-Holland, Amsterdam, 1979), p. 337.

[43] H. Frauenfelder and R. Steffen, in *α-, β-, and γ-Ray Spectroscopy*, edited by K. Siegbahn (North-Holland, Amsterdam, 1968), Vol. 2, p. 917; G. Schatz and A. Weidinger, in *Nuclear Condensed Matter Physics. Nuclear Methods and Applications*, translated by J. A. Gardner (John Wiley & Sons, Chichester, 1996), p. 63.

[44] L. A. Mendoza-Zélis, A. G. Bibiloni, M. C. Caracoche, A. R. López-García, J. A. Martínez, R. C. Mercader, and A. F. Pasquevich, Hyperfine Interact. **3**, 315 (1977).

[45] T. Butz and A. Lerf, Phys. Lett. A **97**, 217 (1983).

[46] Crystal structure data used in PCM predictions. Two references are quoted if lattice parameters and atomic positions come from different articles (lattice parameter articles are quoted first). Sc_2O_3: R. W. G. Wyckoff, *Crystal Structures*, (Wiley Interscience, New York, 1964), Vol. 2; R. Norrestam, Ark. Kemi. **29**, 343 (1968); In_2O_3: M. Marezio, Acta Crystallogr. **20**, 723 (1966); Y_2O_3, Dy_2O_3, and Ho_2O_3: E. N. Maslen, V. A. Streltsov, and N. Ishizawa, Acta Crystallogr. B **52**, 414 (1996); Er_2O_3: see Ref. 33; Yb_2O_3: T. Schleid and G. Meyer, J. Less-Comm. Met. **149**, 73 (1989); Tm_2O_3: H. Ishibashi, K. Shimomoto, and K. Nakahigashi, J. Phys. Chem. Solids **9**, 809 (1994); Lu_2O_3, Eu_2O_3, Gd_2O_3, and Sm_2O_3: S. Stecura and W. Campbell, Thermal Expansion and Phase Inversion of Rare Earth Oxides, Bureau of Mines Report of Investigations N° 5847, U.S. Department of the Interior, 1961; A. Saiki, N. Ishizawa, N. Mizutani, and M. Kato, Yogyo Kyokai Shi **93**, 649 (1985).

[47] P. Herzog, K. Freitag, M. Reuschenbach, and H. Walitzki, Z. Phys. A **294**, 13 (1980).

[48] A. Bartos, K. P. Lieb, M. Uhrmacher, and D. Wiarda, Acta Crystallogr. B **49**, 165 (1993).

[49] V. Vildosola, A. M. Llois, and J. G. Sereni, Phys. Rev. B **69**, 125116 (2004).

[50] S. H. Wei and H. Krakauer, Phys. Rev. Lett. **55**, 1200 (1985).

[51] L. A. Errico, G. Fabricius, and M. Rentería, Hyp. Interact. **136/137**, 749 (2001).

[52] L. A. Errico, G. Fabricius, and M. Rentería, Phys. Stat. Sol. (b) 241, 2394 (2004).

[53] P. Blaha, K. Schwarz, P. Dufek, and J. Luitz, WIEN97, Vienna University of Technology, 1997. Improved and updated Unix version of the original copyrighted WIEN-code, which was published by P. Blaha, K. Schwarz, P.I. Sorantin, and S. B. Trickey, in Comput. Phys. Commun. **59**, 399 (1990).

[54] J. P. Perdew, K. Burke, and M. Ernzerhof, Phys. Rev. Lett. **77**, 3865 (1996).

[55] M. Marezio, Acta Crystallogr. **20**, 723 (1966).

[56] M. Rentería, A. G. Bibiloni, M. S. Moreno, J. Desimoni, R. C. Mercader, A. Bartos, M. Uhrmacher, and K. P. Lieb, J. Phys.: Condens. Matter **3**, 3625 (1991).

[57] M. Rentería, G. N. Darriba, L. A. Errico, and P. D. Eversheim, to be published.